RSC Advances

ROYAL SOCIETY OF CHEMISTRY

www.rsc.org/advances

Journal Name

ARTICLE

Cytotoxic metabolites from the endophytic fungus *Penicillium chermesinum*: Discovery of a cysteine-targeted michael acceptor as a pharmacophore for fragment-based drug discovery, bioconjugation and click reactions†

Received 00th January 20xx,
Accepted 00th January 20xx

DOI: 10.1039/x0xx00000x

www.rsc.org/

Cici Darsih,[a] Vilailak Prachyawarakorn,[b] Suthep Wiyakrutta,[c] Chulabhorn Mahidol,[a,b] Somsak Ruchirawat,[a,b,d] and Prasat Kittakoop [*a,b,d]

Fungal metabolites (**1**-**8**) including known compounds, TMC-264 (**1**), PR-toxin (**6**) and a sesquiterpene (**7**), and new natural products **2**-**5** and **8**, were isolated from the mangrove endophytic fungus *Penicillium chermesinum*. Compound **2** was a novel tetracyclic polyketide uniquely spiro-attached with a γ-lactone ring. Compounds **1** and **6** exhibited comparable cytotoxic activity to that of doxorubicin, and they selectively exhibited the activity toward certain cancer cell lines. The cytotoxicity of **1** might be due to the β-chloro substituted α,β-unsaturated ketone functionality, which was reactive toward glutathione and peptides containing a thiol group. The polyketide **1** reacted with glutathione and peptides under physiological conditions, and its thiol-reactive pharmacophore is possibly applicable to the design of glutathione modulation agents, fragment-based drug discovery (for irreversible enzyme inhibitors), bioconjugation, and click reactions. Facile C-S bond formation in water (catalyst-free condition) inspired by **1** could also be useful for green chemistry.

Introduction

A covalent bond formation between a ligand and a noncatalytic cysteine of a drug target is recently regarded as a powerful strategy in drug discovery,[1, 2] and the recently approved anticancer drugs, afatinib and ibrutinib, are good examples that are successfully designed through a covalent bond formation with a noncatalytic cysteine of kinases.[3, 4] An irreversible covalent bond formation between drugs and targets provide unique therapeutic benefits, for example, longer duration of drug action, greater potency, and preventing drug resistance.[5] While a reversible covalent bond formation of ligands and drug targets is intensively employed in drug discovery,[6-8] an irreversible covalent bond plays a critical role for anticancer drug design of kinase inhibitors; several irreversible kinase inhibitors are under preclinical and clinical evaluations.[9] It is known that natural products provide important pharmacophores for drug discovery, and there are many examples of important drug pharmacophores from natural products. A hydroxamic acid moiety of a natural product trichostatin A is for the inhibition of histone deacetylase (HDAC),[10] and there are several hydroxamic acid HDAC inhibitors including anticancer drugs, vorinostat and suberoylanilide hydroxamic acid (SAHA).[11, 12] A disulfide bond of romidepsin and a thioester moiety of largazole are critical, essential for HDAC inhibitory activity, and the pharmacophores of these natural products have played an important role in anticancer drug development.[13, 14] A spirocyclic cyclopropane of a natural product duocarmycin which is responsible for DNA alkylation properties,[15] and several duocarmycin derivatives are promising anticancer drug candidates.[16, 17] Endophytic fungi or fungal endophytes are microbial plant symbionts, which symbiotically live in plant tissues, and currently they are found to be important sources of bioactive compounds,[18, 19] particularly those isolated from mangrove trees.[20, 21] Here we report the isolation, characterization, and cytotoxic activity of the metabolites (**1**-**8**) (Fig. 1) from the mangrove endophytic fungus *Penicillium chermesinum* strain HLit-ROR2. Among the isolated compounds, the metabolite **2** possessed a novel tetracyclic skeleton uniquely spiro-attached with a γ-lactone ring. Moreover, the reactivity of a cytotoxic natural product toward glutathione (GSH) and peptides is reported, and the application of the thiol-reactive pharmacophore of **1** for the fragment-based drug discovery, bioconjugation, and click reactions is also discussed.

Results and discussion

[a] *Chulabhorn Graduate Institute, Chemical Biology Program, Kamphaeng Phet 6 Road, Laksi, Bangkok 10210, Thailand*
[b] *Chulabhorn Research Institute, Kamphaeng Phet 6 Road, Laksi, Bangkok 10210, Thailand*
[c] *Department of Microbiology, Faculty of Science, Mahidol University, Bangkok 10400, Thailand*
[d] *Center of Excellence on Environmental Health and Toxicology (EHT), CHE, Ministry of Education, Thailand*

† Electronic Supplementary Information (ESI) available: ^{1}H and ^{13}C NMR spectra of new fungal metabolites; and ^{1}H NMR and TOF MS spectra of **1**-GSH adduct (**9**) and **1**-peptide adducts (**10**-**14**). See DOI: 10.1039/x0xx00000x

Structure Elucidation of Fungal Metabolites

Isolation of a broth extract of *P. chermesinum* HLit-ROR2 gave metabolites **1**-**8** including three known compounds, TMC-264 (**1**), PR-toxin (**6**), and eremofortine C derivative (**7**), and five new natural products **2**-**5** and **8** (Fig. 1). It should be noted that **5** was a new natural product, but it was synthetically known, being synthesized during the synthesis of **1**.[22] Spectroscopic data of known compounds **1**, **6**, and **7** were in good agreement with those reported in the literature.[23-25] New compounds **2**-**5** are polyketides and named as "penicilliumolides A-D", while **8** is an eremophilane sesquiterpene.

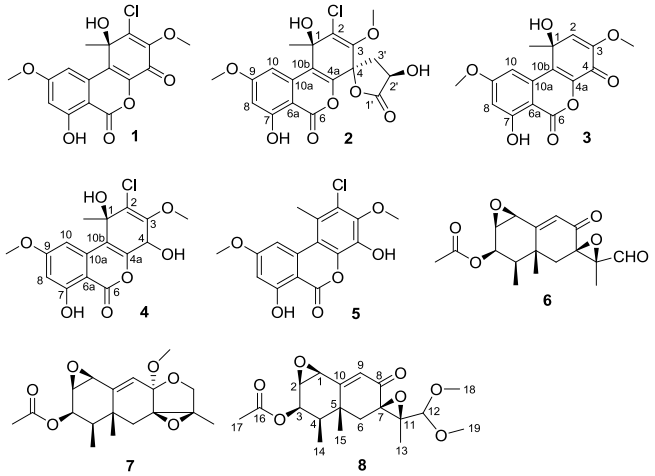

Fig. 1 Structures of fungal metabolites **1**–**8**.

Penicilliumolide A (**2**) had a molecular formula, $C_{19}H_{17}ClO_9$, as deduced from the ESITOF MS spectrum. The presence of one chlorine atom in **2** was evident from the TOF MS isotopic pattern (the ratio of M–H:M–H+2 = 3:1). In general, ^{1}H NMR spectrum of **2** was similar to that of TMC-264 (**1**),[23] except additional signals of H-2' (δ_H 4.90, t, J = 9.1 Hz) and H_2-3' (δ_H 2.84, m) in **2** (Table 1). Compound **2** had ^{1}H NMR signals of *meta*-coupling aromatic protons (H-8 and H-10), 1-Me, two methoxy groups (3-OMe and 9-OMe), and three exchangeable OH protons (1-OH, 2'-OH, and 7-OH), and these signals were typically found in **1**,[23] indicating that **2** shares the same core structure as that of **1**. HMBC spectrum of **2** showed the correlations from 1-Me protons to C-1, C-2, and C-10b; 3-OMe to C-3; 7-OH to C-6 (four-bond correlation), C-7, and C-8; H-8 to C6a, C-7, and C-10; 9-OMe to C-9, H-10 to C-6 (four-bond correlation), C-6a, C-9, and C-10b, and these correlations constructed the core structure, 1-methyl-dibenzo[*b*,*d*]-pyran, of **2**. Careful analysis of ^{13}C NMR revealed that the C-4 ketone in **1** (δ_C 171.9) was replaced by an oxygenated sp^3 quaternary carbon (δ_C 79.5) in **2**, and that **2** had three additional carbons (δ_C 38.0, 68.1, and 175.8). ^{1}H-^{1}H COSY spectrum of **2** showed the correlation of H-2' and H_2-3', while the HMBC spectrum displayed the correlation from H-2' to C-1' and C-4 and from H_2-3' to C-1', C-3, C-4, and C-4a, establishing a structure of five-membered ring spiro-attached to a core structure of TMC-264 (**1**). The absolute configuration 1*R* of TMC-264 (**1**) was

Table 1. ^{1}H and ^{13}C NMR data for compounds **2**, **3**, and **4**.

	2[a]		**3**[b]		**4**[c]	
	δ_H (J in Hz)	δc	δ_H (J in Hz)	δc	δ_H (J in Hz)	δc
1	-	72.2	-	69.6	-	71.9
2	-	127.3	6.04 (s)	123.1	-	121.6
3	-	146.1	-	147.7	-	146.2
4	-	79.5	-	172.5	5.23 (d, 6.7)	63.1
4a	-	143.5	-	141.6	-	148.8
6	-	163.9	-	163.6	-	167.1
6a	-	100.5	-	100.9	-	101.1
7	-	164.5	-	164.2	-	164.8
8	6.59 (d, 1.9)	101.5	6.60 (d, 1.8)	103.1	6.61 (d, 2.3)	100.9
9	-	166.7	-	166.7	-	165.8
10	7.46 (d, 1.9)	106.0	7.66 (d, 1.8)	107.2	7.62 (d, 2.3)	105.1
10a	-	134.8	-	134.1	-	137.4
10b	-	118.5	-	129.9	-	115.9
1'	-	175.8	-	-	-	-
2'	4.90 (t, 9.1)	68.1	-	-	-	-
3'	2.84 (m)	38.0	-	-	-	-
1-Me	1.88 (s)	28.4	1.78 (s)	29.4	1.78 (s)	27.8
3-OMe	3.90 (s)	61.8[d]	3.75 (s)	55.4	3.90 (s)	57.1
9-OMe	3.90 (s)	55.8[d]	3.94 (s)	55.9	3.95 (s)	56.0
1-OH	3.32 (br s)	-	3.15 (br s)	-	5.00 (s)	-
2'-OH	2.80 (br s)	-	-	-	-	-
4-OH	-	-	-	-	5.57 (d, 6.7)	-
7-OH	11.22 (s)	-	11.14 (s)	-	11.53 (s)	-

[a] Acquired in $CDCl_3$ (600 MHz); [b] Acquired in $CDCl_3$ (400 MHz); [c] Acquired in acetone-d_6 (300 MHz); [d] Interchangeable in the same column.

previously established by total synthesis.[22] It is assumed that compound **2** should share the same biosynthetic origin as that of **1**, and thus having 1*R* configuration. The absolute configuration at C-2' in **2** was addressed by Mosher's method; accordingly Mosher's (MTPA) esters **2a** and **2b** were prepared, and the $\Delta\delta$ values ($\delta_{(S)} - \delta_{(R)}$) indicated the *R* configuration for C-2' (Fig. 2). The NOESY spectrum of **2** showed the correlation between H_2-3' and 1-Me protons, suggesting that they were on the same side. Therefore, the C-4 spiro configuration was tentatively assigned to be *S*. Penicilliumolide A (**2**) has a novel tetracyclic skeleton uniquely spiro-attached with a γ-lactone ring.

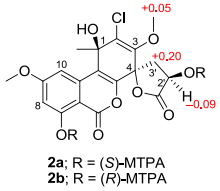

2a; R = (*S*)-MTPA
2b; R = (*R*)-MPTA

Fig. 2 $\Delta\delta$ Values for the MTPA esters **2a** and **2b**.

Penicilliumolide B (**3**), $C_{16}H_{14}O_7$ (by ESITOF MS), had simil... ^{1}H and ^{13}C NMR data (Table 1) to that of TMC-264 (**1**). Detailed

analysis of NMR and MS data revealed that a chlorine atom in **1** was replaced by methine H-2 (δ_H 6.04) in **3**. HMBC spectrum of **3** showed similar correlations to that of **1**, indicating that both shared the same 1*H*-dibenzo[*b*,*d*]pyran-4,6-dione skeleton. The HMBC correlation from H-2 to 1-Me carbon, C-3, C-4, and C-10b assigned the H-2 position in **3**. Compound **3** should share the same biosynthetic origin as that of TMC-264 (**1**), therefore the configuration of 1-OH in **3** should be the same as that of **1**.

ESITOF MS analysis of penicilliumolide C (**4**) returned a molecular formula of $C_{16}H_{15}ClO_7$. Again, ^{1}H and ^{13}C NMR data of **4** shared a great deal of similarities to that of TMC-264 (**1**), showing signals of two aromatic protons (H-8 and H-10), two methoxy groups (3-OMe and 9-OMe), 1-Me, and three exchangeable OH protons (1-OH, 4-OH, and 7-OH). The only difference was that **4** has additional signals of H-4 (δ_H 5.23) and 4-OH (δ_H 5.57); ^{1}H-^{1}H COSY spectrum showed the correlation between these two protons. Positions of H-4 and 4-OH were assigned by the HMBC correlations from H-4 to C-2, C-3, C-4a, and C-10b, and from 4-OH to C-3 and C-4. On the basis of these spectroscopic data, the structure of **4** was secured. Attempt to clarify the C-4 configuration in **4** was carried out using Mosher's method, however, the Mosher's esters were not obtained because of the instability of the ester products.

Penicilliumolide D (**5**), $C_{16}H_{13}ClO_6$, was a new natural product, but it was synthetically known, being a key synthetic intermediate of **1**; previously, Tatsuta and co-workers demonstrated that oxidation of **5** by salcomine under oxygen atmosphere gave (±)-TMC-264 (**1**).[22] As **5** was co-isolated with **1** from the same fungus, the metabolite **5** is possibly a biosynthetic intermediate of **1**.

Compound **8** had a molecular formula, $C_{19}H_{26}O_7$, as deduced from ESITOF MS, and its ^{1}H and ^{13}C NMR data were similar to that of PR-toxin (**6**).[24] Detailed analysis of NMR data revealed that an aldehydic signal in **6** was replaced by two methoxy groups in **8**, suggesting that an aldehyde in **6** was transformed to an acetal group in **8**. Position of the two methoxy groups in **8** was assigned by HMBC correlations from both 18-OMe and 19-OMe to C-12. However, as an acetal is normally derived from aldehyde under acidic condition, compound **8** is possibly an artifact derived from **6** during purification by silica gel.

Cytotoxic Activity of Fungal Metabolites

Cytotoxic activity of the isolated compounds **1**-**8** was evaluated. Compounds **1** and **6** displayed cytotoxic activity, while other compounds (**2**-**5**, **7**, and **8**) were inactive or exhibited only weak activity toward particular cell lines (Table 2). It is worth mentioning that the activities of **1** and **6** towards some cell lines were comparable to that of the standard anticancer drug, doxorubicin, for example, the activity of **1** against T47D (IC_{50} 1.08 μM) and MDA-MB231 (IC_{50} 2.81 μM) cancer cell lines comparable to that of doxorubicin (IC_{50} 1.55 and 2.24 μM for T47D and MDA-MB231, respectively). Interestingly, the cytotoxic activity (IC_{50} 3.27 μM) of **1** against HepG2 cell line was *ca* 11 times more potent than that (IC_{50} 35.66 μM) of etoposide, an anticancer drug (Table 2). In addition, compound **1** selectively exhibited cytotoxic activity toward MOLT-3 (IC_{50} 1.36 μM) and T47D (IC_{50} 1.08 μM) cancer cell lines with the selectivity index (SI) values of 9 and 11, respectively (IC_{50} 12.64 μM for normal cell line, MRC-5). The SI value is the ratio of IC_{50} of normal cell (MRC-5)/IC_{50} of cancer cell line. The activity (IC_{50} 0.81–2.19 μM) of PR-toxin (**6**) toward HuCCA-1, HeLa, T47D, and MDA-MB231 cell lines was comparable to that of doxorubicin (IC_{50} 0.26–2.24 μM) (Table 2). Interestingly, the activity (IC_{50} 0.06 μM) of **6** against HL-60 cell line was more potent than doxorubicin (IC_{50} 1.21 μM), and compound **6** selectively exhibited cytotoxic activity against MOLT-3 (IC_{50} 0.09 μM) and HL-60 (IC_{50} 0.06 μM) cell lines with respective SI values of 40 and 61 (IC_{50} 3.66 μM for MRC-5 cell line). Although PR-toxin (**6**) is a known mycotoxin, inhibiting the transcriptional process in liver cells,[26] its cytotoxic activity against cancer cell lines has never been yet demonstrated. Compounds **7** and **8** were derivatives of **6**, lacking of an aldehyde group; they were relatively non-toxic towards cell lines tested, suggesting that the aldehyde functionality of **6** was important for cytotoxic activity.

Reactivity of 1 toward GSH and Peptides

As compound **1** exhibited potent cytotoxic activity, its structural feature was therefore of interest for such biological activity. While **1** exhibited potent cytotoxic activity, its derivatives **2**–**5** were inactive or showed only weak activity against some cell lines (Table 2); this suggested that the β-chloro substituted α,β-unsaturated ketone of **1** might be responsible for the activity. It is known that α,β-unsaturated carbonyl compounds are of pharmaceutical interests, having potential Michael acceptor activity, and they possess several biological activities.[27] Among them, α,β-unsaturated carbonyl was essential for the inhibition of tyrosinase and angiotensin converting enzyme (ACE).[28] Previously, the glutathione (GSH)-reactive α,β-unsaturated carbonyl agent was identified as a drug metabolite of mercaptopurine, an immunosuppressive drug,[29] later GSH-reactive analogs were designed, showing a significant cytotoxic activity against murine melanoma cell line, and they were potential agents targeting tumors containing a high concentration of GSH.[30] Although GSH is important for cell survival, many studies reveal that it could promote cancer, and thus impeding cancer chemotherapy, therefore glutathione modulation and depletion could be applied to cancer therapy.[31, 32] The reactivity of **1** with GSH was therefore investigated in this study.

Compound **1** (1.0 mg, 2.83 μmol; 1 equiv.) was incubated with GSH (1.7 mg, 5.53 μmol; 2 equiv.) in 0.1 M phosphate buffer (pH 7.0) containing 20% (v/v) of EtOH; a total volume of a solvent was 2 mL. Addition of EtOH to the reaction mixture increased the solubility of **1** in the buffer. HPLC analysis revealed that **1** completely reacted with GSH within 2 h; the 1-GSH adduct (**9**) was obtained after HPLC purification. The adduct **9** was yellow solid, and its ^{1}H NMR spectrum (CD_3OD) showed typical signals of **1** (i.e. δ_H 6.73 and 7.75 for H-8 and H-10, and δ_H 3.88, 3.93, and 1.91 for 9-OMe, 3-OMe and 1-Me, respectively) and GSH (i.e. δ_H 3.49-3.81 for α-protons, 2.0[illegible],

and 2.50) (Fig. 1SA, ESI). The ESITOF MS spectrum revealed the molecular formula, $C_{26}H_{29}N_3NaO_{13}S$, for **1**-GSH adduct (**9**), showing the ion peaks at *m/z* 624.1496 of $[M+H]^+$ (calcd for $C_{26}H_{30}N_3O_{13}S$, 624.1499) and 646.1290 of $[M+Na]^+$ (calcd for $C_{26}H_{29}N_3NaO_{13}S$, 646.1319). The formation of **1**-GSH adduct (**9**) is proposed in Fig. 3. The reaction of **1** and GSH is possibly through a conjugate addition-elimination reaction. First, the addition of the thiol of GSH to **1** takes place, leading to the enol intermediate **A**. Instead of the reverse loss of the thiol, the chlorine atom is eliminated, leaving the thiol attached.

Table 2. Cytotoxic activity of compounds **1**-**8**

Compound	Cytotoxic activity (IC_{50}, μM); mean ± s.d., *n* = 3								
	HuCCA-1	HepG2	A549	MOLT-3	HeLa	T47D	HL-60	MDA-MB231	MRC-5
1	5.62±0.11	3.27±0.11	8.01±1.76	1.36±0.14	4.49±1.14	1.08±0.03	ND	2.81±0.23	12.64±1.02
2	IA	IA	IA	IA	ND	ND	ND	ND	ND
3	103.02±2.36	IA	IA	9.03±3.62	ND	ND	ND	ND	ND
4	IA	IA	IA	69.55±9.60	ND	ND	ND	ND	ND
5	IA	IA	IA	55.98±1.52	ND	ND	ND	ND	ND
6	0.81±0.03	3.41±0.47	8.59±0.19	0.09±0.003	1.22±0.16	1.00±0.13	0.06±0.03	2.19±0.19	3.66±0.59
7	IA	IA	IA	IA	ND	ND	ND	ND	ND
8	IA	IA	IA	90.82±18.85	IA	IA	ND	IA	IA
Doxorubicin	0.77±0.16	0.45±0.07	0.31±0.09	ND	0.26±0.03	1.55±2.43	1.21±0.05	2.24±0.31	IA
Etoposide	ND	35.66±1.00	ND	0.03±0.002	ND	ND	ND	ND	ND

Doxorubicin and etoposide were standard anticancer drugs. IA = Inactive at 50 μg/mL; ND = Not determined; HuCCA-1 = human cholangiocarcinoma cell line; HepG2 = human hepatocellular carcinoma cell line; A549 = human lung adenocarcinoma cell line; MOLT-3 = human acute T-lymphoblastic leukemia cell line; HeLa = human cervical carcinoma cell line; T47D = hormone-dependent human breast cancer cell line; HL-60 = human promyelotic leukemia cell line; MDA-MB-231= hormone-independent human breast cancer cell line; MRC-5 = normal human embryonic lung fibroblasts.

Although **1** reacted with GSH, its derivatives (**3**–**5**) did not react with GSH; this supports that the β-chloro substituted α,β-unsaturated ketone of **1** is critical for the reaction, and thus conferring the cytotoxic activity of **1**. Despite the fact that an eremophilane-type sesquiterpene **6** exhibited potent cytotoxic activity, it could not react with GSH, suggesting that this compound class exerts the activity through other mechanisms of action, not a cysteine-targeted Michael acceptor.

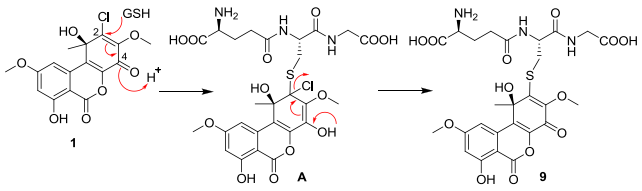

Fig. 3 Proposed mechanism for the formation of **1**-GSH adduct (**9**).

It is anticipated that, in addition to GSH, compound **1** may react with cysteine containing biomolecules (proteins). Therefore, the reaction of **1** and peptides containing cysteine was subsequently investigated. Five peptides with 8-9 amino acid residues were used as models; they were Ile-Gly-Ser-Thr-Phe-Leu-Cys-Ser-Leu (peptide I); Ile-Tyr-Ala-Cys-Leu-Gly-Pro-Gly (peptide II); Tyr-Leu-Cys-Thr-Gly-Leu-Ala-Ser-Ile (peptide III); Gly-Leu-Phe-Thr-Ala-Leu-Cys-Ser-Leu (peptide IV); and Ile-Leu-Ser-Thr-Phe-Leu-Gly-Ser-Cys (peptide V). The reaction of **1** and peptides was performed using the stoichiometric ratio of 1:2 for **1** and individual peptide. Compound **1** (*ca* 1.0 mg, 2.83 μmol) was incubated with each peptide in 0.1 M phosphate buffer (with 20% of EtOH), pH 7.0. Progress of a reaction was monitored by HPLC. Indeed, **1** reacted with peptides I-V, however, it showed different reactivity toward individual peptide. The reaction of **1** with the peptide II was nearly complete after 2 h (with 1% of unreacted substrate **1**), while that with the peptides I and III were nearly complete after 6 and 4 h (each with 3% of unreacted substrate **1**), respectively; this suggested that the reactivity of **1** toward the peptide II was much greater than that of the peptides I and III. The peptides IV and V had less reactivity than other peptides with 18-19% of unreacted substrate **1** after 6-h incubation. After the reaction, **1**-peptide adducts (**10**-**14**) (Fig. 4) were individually purified by HPLC. The **1**-peptide adduct (**10**) was obtained (0.5 mg) after HPLC purification, and its ^{1}H NMR spectrum (Fig. 1SB, ESI) displayed signals of **1** and peptide I. The characteristic signals for **1** included δ_H 6.72 and 7.77 for H-8 and H-10, and δ_H 3.87, 3.92, and 1.89 for 9-OMe, 3-OMe and 1-Me, respectively, while the signals for peptide I could be observable, for example, δ_H 7.10-7.30 for aromatic protons of Phe, δ_H 3.50-4.70 for α-protons and protons attached to an oxygen atom of Ser and Thr, and δ_H 0.80-1.00 for methyl protons of Leu and Ile (Fig. 1SB, ESI). The ESITOF MS spectrum indicated the molecular formula $C_{58}H_{81}N_9O_{20}S$ for **1**-peptide adduct (**10**), showing the ion peak at *m/z* 1256.5410 of $[M+H]^+$ (calcd for $C_{58}H_{82}N_9O_{20}S$, 1256.5397).

The **1**-peptide adducts (**11**-**14**) were prepared and characterized in the same manner as that of the adduct **10**. The ^{1}H NMR spectrum of the adduct **11** showed signals of **1**, i.e., δ_H 6.70 (overlapping with aromatic protons of Tyr) and 7.78 for H-8 and H-10, and δ_H 3.89, 3.94, and 1.91 for 9-OMe, 3-OMe and 1-Me, respectively (Fig. 1SC, ESI), as well as signals of peptide II, for example, δ_H 6.70 and 7.08 for aromatic protons of Tyr, δ_H 3.50-4.80 for α-protons, and δ_H 0.80 and

0.95 for methyl protons of Ile and Leu. The molecular formula $C_{52}H_{68}N_8O_{17}S$ for **11** was deduced from the ESITOF MS spectrum, displaying the ion peak at *m/z* 1109.4525 of $[M+H]^+$ (calcd for $C_{52}H_{69}N_8O_{17}S$, 1109.4501). The ^1H NMR spectrum of the adduct **12** showed similar signals to that of the adduct **11**, for example, the signals for compound **1** (δ_H 6.74, 7.79, 3.87, 3.93, and 1.90 for H-8, H-10, 9-OMe, 3-OMe, and 1-Me, respectively) and for peptide (i.e., δ_H 6.74 and 7.00 for aromatic protons of Tyr, 3.50-4.70 for α-protons, and 0.80-1.00 for methyl protons of Leu and Ile). The ESITOF MS spectrum of the adduct **12** revealed the molecular formula $C_{58}H_{81}N_9O_{20}S$, exhibiting the ion peak at *m/z* 1256.5423 of $[M+H]^+$ (calcd for $C_{58}H_{82}N_9O_{20}S$, 1256.5397). The adducts **13** and **14** were prepared from the peptides containing Phe residue, therefore, their ^1H NMR spectra displayed the typical signal of aromatic protons of Phe at δ_H 7.18-7.35 for aromatic protons of Phe (ESI), which was similar to that of the adduct **10**. The signals for α-protons and methyl protons of Leu and Ile

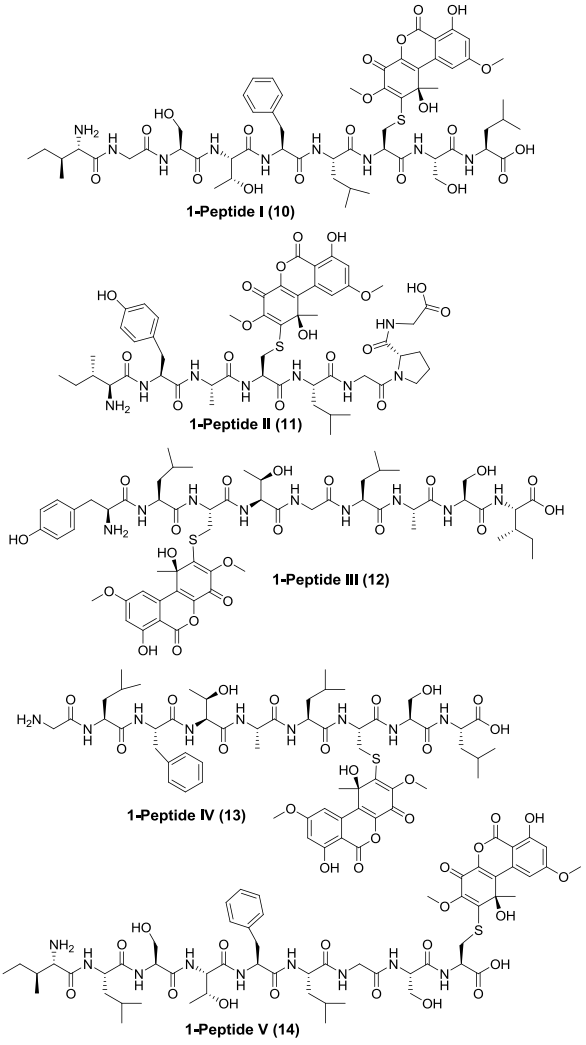

Fig. 4 Structures of **1**-peptide adducts (**10**-**14**).

were also observed. The ESITOF MS spectrum established the molecular formula $C_{58}H_{81}N_9O_{19}S$ for **1**-peptide adduct (**13**), showing the ion peak at *m/z* 1240.5500 of $[M+H]^+$ (calcd for $C_{58}H_{82}N_9O_{19}S$, 1240.5448). The molecular formula for **1**-peptide adduct (**14**) was established as $C_{58}H_{81}N_9O_{20}S$ by the ESITOF MS spectrum, observed *m/z* 1256.5398 of $[M+H]^+$ (calcd for $C_{58}H_{82}N_9O_{20}S$, 1256.5397).

These experiments demonstrated that TMC-264 (**1**) was reactive toward GSH and peptides with a cysteine residue; it is therefore possible that the cytotoxic activity of **1** could be partly due to such reactivity. The reactivity of **1** toward GSH and peptides containing cysteine was through the reaction of the β-chloro substituted α,β-unsaturated ketone with a thiol group. The reactive pharmacophore of **1** could therefore be useful for the design of glutathione modulation agents, as well as the design of inhibitors for irreversible enzyme inhibition, e.g., kinase and protease inhibitors. The modulation and depletion of glutathione are known to be useful for cancer therapy,[31, 32] and a covalent bond formation between a ligand and a noncatalytic cysteine of a drug target is known to be one of the efficient strategies in drug discovery.[1, 2] Moreover, a covalent bond between small molecules and a specific cysteine of protein target also plays an important role of "targeted covalent drugs", which have been applied to making drug candidates, especially for kinases inhibitors.[33] Fragment-based drug discovery is recently recognized as a powerful approach for drug discovery and chemical biology,[34] and the reactive pharmacophore of **1** toward a thiol group may be valuable for such approach. The recent achievement employing the thiol-reactive pharmacophore in the fragment-based drug discovery is the discovery of irreversible covalent inhibitors of cysteine proteases.[35] Bioconjugation has recently played a great role in chemical biology, particularly in the field of medicine and biomaterials, for example, modification of proteins for the generation of protein-based materials.[36, 37] The present work already demonstrated that TMC-264 (**1**) reacted with the peptides containing cysteine under mild conditions, therefore, the reactive scaffold of **1** may be applied to bioconjugation research.

The chemistry of the β-chloro substituted α,β-unsaturated ketone in **1** toward thiol containing compounds, e.g., GSH and peptides containing cysteine, is interesting because it could undergo under mild conditions (in catalyst-free aqueous solution), which could be employed for click chemistry of thiol containing compounds. Normally, thiol-ene and thiol-yne click reactions are one of the popularly known click reactions, and have been utilized in many research areas, for example, materials, biomolecular, and macromolecular chemistry, as well as drug delivery research.[38] However, thiol-ene and thiol-yne click reactions require catalysts under relatively strong reaction conditions, for example, under basic conditions with a radical initiator α,α-dimethoxy-α-phenylacetophenone (DMPA)[38a] and using 2,2-dimethoxy-2-phenyl-acetophenone (DPAP) as radical initiator and 4-methoxyacetophenone (MAP) as a photosensitizer.[38b] These conditions could not be utilized in biological systems in which most biomolecules are likely degraded by reagents and basic conditions. The β-chloro substituted α,β-unsaturated ketone functionality in **1** may serve as a new thiol-reactive group for click reactions that could be performed in a catalyst-free aqueous solution or

under physiological conditions. The reaction reported here occurs in aqueous solution and at room temperature, which is ideal for click reactions of biomolecules. Some reactions in organic chemistry were inspired by natural products, for example, nitrone formation in aqueous solutions and dimerisation of prenylated quinones.[39] Mild and general methods for C-S bond formation have recently received great attention because the C-S bond is present in several biological and pharmaceutical compounds.[40] The facile C-S bond formation guided by the thiol-reactive group in **1** is a new reaction inspired by a natural product, and this reaction may be useful for organic chemistry, particularly for the chemical synthesis employing green chemistry approaches. It is worth mentioning that TMC-264 (**1**) was previously reported as an antiallergic agent, exhibiting potent inhibitory activity against tyrosine phosphorylation of STAT6.[23, 41]

Experimental

General Methods

^{1}H, ^{13}C, DEPT 90, DEPT 135, HMQC, HMBC, COSY, and NOESY spectra were recorded either on 300, or 400, or 600 MHz NMR spectrometers. ESITOF MS spectra were obtained from electrospray ionization time-of-flight mass spectrometer. IR spectra were obtained from FTIR spectrophotometer. Separation by high performance liquid chromatography (HPLC) was performed using a photodiode array detector. Column chromatography was carried out using either silica gel (0.063-0.200 mm) or Sephadex LH-20 as packing materials.

Identification of HLit-ROR2 Fungus

The endophytic fungus *Penicillium chermesinum* strain HLit-ROR2 was isolated from a root of a mangrove tree, *Hertiera littoralis*, which was collected on November 2012 from the Mangrove Forest Learning and Development Center 2, Samut Sakhon province, Thailand. The HLit-ROR2 fungus was identified based on morphological characteristics and the analysis of DNA sequences of the ITS1-5.8S-ITS2 ribosomal RNA gene region.

Morphological Characterization. The HLit-ROR2 fungus was inoculated in three-point fashion on malt extract agar (MEA) in 90 mm plastic Petri dishes. Plates were incubated at 30 °C, in darkness. Colony characters were examined after 7 and 14 d of incubation. For microscopic observations, slides were prepared from 10 d old colonies on MEA.[42] After 7 d incubation on MEA at 30 °C, the HLit-ROR2 fungus grew to colony diameter of 32 ± 0.8 mm. Colonies were flat, raised at the center, conidiogenesis was moderate to heavy, appearing as finely granulate, dull grey area; exudate absent; colony margin low, narrow, entire, effuse. The reverse side colony color was dull cream. At 14 d old, the colony turned dull greyish-blue obverse, and orange-brown reverse. Microscopic structures: conidiophores borne on aerial mycelium; stipes septate, smooth-walled; monoverticillate; phialides ampulliform. Conidia smooth-walled, ellipsoidal, 1.5 × 2.5 µm.

DNA Sequence-Based Identification. The HLit-ROR2 fungus was cultivated in malt extract broth for 5 d, the mycelium was collected and washed with sterile water. Cellular DNA was extracted from the washed fungal mycelium using the DNA kit. The ITS1-5.8S-ITS2 of the ribosomal RNA gene region was amplified from the fungal genomic DNA by PCR using the ITS5 (GGAAGTAAAAGTCGTAACAAGG) and ITS4 (TCCTCCGCTTATTGATATGC) primers.[43] The thermal cycle program was as follows: 5 min at 95 °C followed by 30 cycles of 50 s at 95 ºC, 40 s at 45 ºC and 60 s at 72 ºC, with a final extension period of 10 min at 72 ºC. The amplified DNA fragment was purified and subjected to DNA sequencing on both strands using primers ITS5 and ITS4. The DNA sequence of the complete ITS1-5.8S-ITS2 (508 nucleotides) was submitted to the online BLASTN 2.2.30+[44] to search for similar sequences in GenBank. The DNA sequences from type strains were selected for alignment using the ClustalW multiple sequence alignment program in the CLC Main Workbench software package version 6.6.2 with manual final adjustment. Phylogenetic relationship was estimated using the neighbor-joining method. Bootstrap analysis was performed with 1000 replications to determine the support for each clade.

BLAST search of the ITS1-5.8S-ITS2 DNA sequence revealed that the HLit-ROR2 was related to fungi in the genus *Penicillium*. Highly similar ITS1-5.8S-ITS2 DNA sequences from 9 reference fungal type strains having 5.8S identical to that of the HLit-ROR2 were retrieved for constructing a phylogenetic tree. The HLit-ROR2 fungus clustered with *Penicillium chermesinum* CBS 231.81, a type strain fungus, with 100 % ITS1-5.8S-ITS2 sequence identity (Figure 2S, ESI). The next closely related fungi were *P. indicum* CBS 115.63 and *P. gerundense* CBS 179.81 both with 98.18 % sequence identity (Figure 1S). Six other ingroup related fungi had 92.09 – 94.77 % sequence identity with the HLit-ROR2.

Based on morphological characteristics and phylogenetic analysis with reference to current taxonomy of the genus *Penicillium*,[45-47] this fungus was identified as *Penicillium chermesinum* HLit-ROR2. DNA sequence data of ITS1-5.8S-ITS2 rRNA gene region of the HLit-ROR2 fungus has been deposited in GenBank with an accession number of KR076794. Culture of the HLit-ROR2 has been deposited at Chulabhorn Research Institute.

Fungal Cultivation, Extraction, and Isolation of Compounds 1-8

The fungus *P. chermesinum* was grown on potato dextrose agar (PDA) for nine days and then cultivated into 1-L Erlenmeyer flasks (40 flasks), each flask containing 250 mL of potato dextrose broth (PDB) and incubated for 31 days at room temperature. Mycelia and broth were then separated by filtration, and broth was extracted three times, each with an equal volume of EtOAc, to give a broth extract (3.24 g). The crude broth extract was first fractionated by Sephadex LH-20 column chromatography (CC) (83 cm x 3 cm) eluted with 100% MeOH to yield 11 fractions (F1-F11). Fraction F8 was purified by reversed-phase HPLC (C18 column, 25 cm x 21.2 mm, 50 % MeOH/H_2O, a flow rate of 12 mL min^{-1}) to give 6 fractions (A1-A6). Faction A5 was identified as TMC-264 (**1**, 30.2 mg). Fractions A4 and A6 were individually separated by Sephadex LH-20 CC (1.5 x 40 cm), eluted with MeOH, to afford

compounds **3** (10.3 mg) and **2** (6.4 mg), respectively. Crystallization (from MeOH) of fraction F9 gave compound **5** (7.6 mg).

Fraction F4 was further purified by silica gel CC (3 x 28 cm), eluted with gradient solvent systems of CH_2Cl_2/EtOAc (100:0 to 0:100) and EtOAc/MeOH (95:5 to 90:10), to afford 12 fractions (B1-B12). Fractions B2 and B3 were combined and identified as PR-toxin (**6**) (690.6 mg). Fraction B-5 was separated by reversed-phase HPLC (C18 column, 19 cm x 250 mm, 50% MeOH/H_2O, a flow rate of 12 mL min^{-1}), yielding compound **7** (23.3 mg). Fraction B6 was purified by PTLC developed with a solvent system of CH_2Cl_2:EtOAc (65:35) to give compound **8** (23.0 mg).

Compound **4** was isolated from a broth extract of the fungus *P. chermesinum* which was cultivated on Czapex medium. The fungus HLit-ROR2 was cultivated into 1-L Erlenmeyer flasks (16 flasks), each flask containing 250 mL of Czapex medium, and incubated for 31 days at room temperature. Mycelia and broth were separated by filtration, and broth was extracted three times, each with an equal volume of EtOAc, to give a broth extract (319.7 mg). The crude broth extract was purified using Sephadex LH-20 CC (110 cm x 2 cm), eluted with MeOH, to give 12 fractions. Fraction 8 was purified by reversed-phase HPLC (C18 column, 25 cm x 21.2 mm, MeCN/H_2O (30-100%), a flow rate of 10 mL min^{-1}), yielding compound **4** (11.9 mg).

*Compound **2**:* Pale yellow solid; $[\alpha]_D^{26}$= −16.7 (*c* 0.48, $CHCl_3$); ^1H and ^{13}C NMR data, see Table 1, FTIR (ATR) ν_{max} cm^{-1}: 3421, 2920, 2850, 1789, 1688, 1673, 1618, 1574, 1242, 1204, 1164, 1096, 1023, 945, 860, 798, 745; UV (MeOH) λ_{max} nm (log ε): 202 (4.3), 247 (4.5), 332 (3.7); ESITOF MS: *m/z* 423.0487 $[M-H]^-$ (calcd for $C_{19}H_{16}ClO_9$, 423.0483).

*Compound **3**:* Pale yellow solid; $[\alpha]_D^{27}$= −85.8 (*c* 0.91, $CHCl_3$); ^1H and ^{13}C NMR data, see Table 1; FTIR (ATR) ν_{max} cm^{-1}: 3483, 2963, 1677, 1257, 1094, 1015, 791; UV (MeOH) λ_{max} nm (log ε): 234 (4.8), 264 (4.7), 349 (4.3); ESITOF MS: *m/z* 317.0655 $[M-H]^-$ (calcd for $C_{16}H_{13}O_7$, 317.0661).

*Compound **4**:* Pale yellow solid; $[\alpha]_D^{27}$= −42.7 (*c* 0.78, acetone); ^1H and ^{13}C NMR data, see Table 1; FTIR (ATR) ν_{max} cm^{-1}: 3306, 3144, 2941, 1686, 1619, 1569, 1323, 1256, 1159, 1075, 965, 738; UV (MeOH) λ_{max} nm (log ε): 246 (4.7), 279 (3.8), 289 (3.7), 330 (3.9); ESITOF MS: *m/z* 355.0578 $[M+H]^+$ (calcd for $C_{16}H_{16}ClO_7$, 355.0585).

*Compound (**8**):* White solid; $[\alpha]_D^{27}$= +201.5 (*c* 1.08, $CHCl_3$); UV (MeOH) λ_{max} nm (log ε): 245 (4.3); FTIR (ATR) ν_{max} cm^{-1}: 2967, 2935, 1743, 1682, 1246, 1105, 1079; ^1H NMR ($CDCl_3$, 300 MHz) δ 6.38 (1H, s, H-9), 5.11 (1H, t, *J* = 5.1 Hz, H-3), 4.88 (1H, s, H-12), 3.88 (1H, dd, *J* = 3.6, 4.8 Hz, H-2), 3.61 (1H, d, *J* = 3.5 Hz, H-1), 3.52 (3H, s, 19-OMe), 3.34 (3H, s, 18-OMe), 2.12 (3H, s, 17-Me), 2.11 (1H, d, *J* = 14.4 Hz, H-6b), 1.83 (1H, d, *J* = 14.6 Hz, H-6a), 1.76 (1H, m, H-4), 1.36 (3H, s, 13-Me), 1.30 (3H, s, 15-Me), 0.98 (3H, d, *J* = 7.1 Hz, 14-Me); ^{13}C NMR ($CDCl_3$, 75 MHz) δ 193.2 (C, C-8), 170.6 (C, C-16), 161.4 (C, C-10), 131.3 (CH, C-9), 104.6 (CH, C-12), 69.9 (CH, C-3), 67.5 (C, C-11), 60.5 (C, C-7), 56.9 (CH_3, 19-OMe), 56.2 (CH_3, 18-OMe), 55.8 (CH, C-1), 55.2 (CH, C-2), 42.1 (CH, C-4), 41.8 (CH_2, C-6), 37.3 (C, C-5), 22.5 (CH_3, C-15), 20.6 (CH_3, C-17), 11.6 (CH_3, C-13), 10.3 (CH_3, C-14); ESITOF MS: *m/z* 389.1588 $[M+Na]^+$ (calcd for $C_{19}H_{26}NaO_7$, 389.1576).

Synthesis of (*R*) and (*S*)-MTPA Esters of Compound 2

To compound **2** (3.2 mg) in NMR tube, (*R*)-(−)-α-methoxy-α-(trifluoromethyl)phenylacetyl chloride (20 μL) and pyridine-d_5 (0.5 mL) were added. The reaction was shaken vigorously, and monitored by TLC and ^1H NMR spectrum. The reaction mixture was purified by PTLC developed with a solvent of CH_2Cl_2:MeOH (79:1), yielding (*S*)-MTPA ester **2a**. In addition, (*R*)-MTPA ester **2b** was prepared in the same manner as that of (*S*)-MTPA ester.

*(S)-MTPA Ester **2a**:* ^1H-NMR ($CDCl_3$, 600 MHz) δ_H: 8.00 (1H, d, *J* = 2.4 Hz, H-10), 6.70 (1H, d, *J* = 2.4 Hz, H-8), 6.07 (1H, t, *J* = 9.3 Hz, H-2'), 3.97 (3H, s, 3-OCH_3), 3.91 (3H, s, 9-OCH_3), 2.94 (2H, m, H-3'), 1.90 (3H, s, CH_3-1), ESI-TOF MS: *m/z* 879.1260 $[M+Na]^+$ (calcd for $C_{39}H_{31}ClF_6NaO_{13}$, 879.1255).

*(R)-MTPA Ester **2b**:* ^1H-NMR ($CDCl_3$, 600 MHz) δ_H: 7.94 (1H, d, *J* = 2.4 Hz, H-10), 6.63 (1H, d, *J* = 2.4 Hz, H-8), 6.16 (1H, t, *J* = 9.4 Hz, H-2'), 3.92 (3H, s, 3-OCH_3), 3.85 (3H, s, 9-OCH_3), 2.74 (2H, m, H-3'), 1.88 (3H, s, CH_3-1), ESI-TOF MS: *m/z* 879.1239 $[M+Na]^+$ (calcd for $C_{39}H_{31}ClF_6NaO_{13}$, 879.1255).

Preparation of 1-GSH Adduct (9)

Glutathione (1.7 mg, 2 equiv.) was dissolved in a mixture of 0.1 M phosphate buffer (pH 7.0) and EtOH (4:1; a total volume was 2 mL). To a solution of glutathione, TMC-264 (**1**) (1.0 mg, 1 equiv.) was added; the reaction mixture was stirred at room temperature. Progress of the reaction was monitored by reversed-phase HPLC analysis. The reaction was complete after 2 h, then it was purified by reversed-phase HPLC (C18 column, 25 cm x 21.2 mm, gradient elution using MeOH/H_2O (20-100% MeOH) in 60 min, a flow rate of 10 mL min^{-1}), yielding 2.0 mg of **1**-GSH adduct (**9**) (t_R 16.5 min).

*1-GSH Adduct (**9**):* ^1H NMR (CD_3OD, 300 MHz): characteristic signals for **1**, δ_H 7.75, 6.73, 3.93, 3.88, and 1.91; characteristic signals for GSH, δ_H 3.49-3.81, 2.50, and 2.08; ESITOF MS: *m/z* 624.1496 $[M+H]^+$ (calcd for $C_{26}H_{30}N_3O_{13}S$, 624.1499), and *m/z* 646.1290 $[M+Na]^+$ (calcd for $C_{26}H_{29}N_3NaO_{13}S$, 646.1319).

Preparation of 1-Peptide Adducts (10-14)

The reaction of **1** and peptides I-V was carried out in the same manner as that for the preparation of **1**-GSH adduct (**9**). TMC-264 (**1**) (*ca* 1.0 mg, 2.83 μmol, 1 equiv.) was incubated with each peptide (*ca* 4.5-5.3 mg, 2 equiv.) in 0.1 M phosphate buffer, pH 7.0 (with 20% of EtOH); a total volume was 2 mL. As revealed by reversed-phase HPLC analysis, there were 3%, 18%, and 19% of unreacted substrate **1** after 6 h-incubation of peptides I, IV, and V with compound **1**. There were 1% and 3% of unreacted **1** after incubation of **1** and peptides II and III for 2 and 4 h, respectively. After incubation of **1** and peptides I-V for certain time as indicated earlier, the adducts **10**-**14** were purified by reversed-phase HPLC (a flow rate of 10 mL min^{-1}), eluted with a gradient system: MeCN/H_2O from 30% to 100% MeCN in 60 min for the adduct **10**; MeOH/H_2O from 30% to 100% MeOH in 60 min for **11**; MeOH/H_2O from 35% to 100 %

MeOH in 60 min for **12**; MeOH/H_2O from 40% to 100% MeOH in 60 min for **13**; and MeOH/H_2O from 45% to 100% MeOH in 60 min for **14**. Under these HPLC conditions, **1**-peptide adducts (**10**-**14**) had t_R of 16.2, 33.9, 36.0, 44.9, and 35.0 min, respectively, and yields of the adducts **10**-**14** were 0.5, 1.9, 1.0, 0.9, and 0.5 mg, respectively.

*1-Peptide Adduct (**10**):* ^{1}H NMR (CD_3OD, 300 MHz): characteristic signals for **1**, δ_H 7.77, 6.72, 3.92, 3.87, and 1.89; characteristic signals for peptide, δ_H 7.10-7.30, 3.50-4.70, 1.40-1.80, and 0.80-1.00; ESITOF MS: *m/z* 1256.5410 $[M+H]^+$ (calcd for $C_{58}H_{82}N_9O_{20}S$, 1256.5397).

*1-Peptide Adduct (**11**):* ^{1}H NMR (CD_3OD, 300 MHz): characteristic signals for **1**, δ_H 7.78, 6.70, 3.94, 3.89, and 1.91; characteristic signals for peptide, δ_H 7.08, 6.70, 3.50-4.80, 2.80-3.20, 1.90-2.20, 1.68, 1.10-1.47, 0.95, and 0.80; ESITOF MS: *m/z* 1109.4525 $[M+H]^+$ (calcd for $C_{52}H_{69}N_8O_{17}S$, 1109.4501).

*1-Peptide Adduct (**12**):* ^{1}H NMR (CD_3OD, 300 MHz): characteristic signals for **1**, δ_H 7.79, 6.74, 3.93, 3.87, and 1.90; characteristic signals for peptide, δ_H 7.00, 6.74, 3.50-4.70, 1.60, 1.10-1.52, and 0.80-1.00; ESITOF MS: *m/z* 1256.5423 $[M+H]^+$ (calcd for $C_{58}H_{82}N_9O_{20}S$, 1256.5397).

*1-Peptide Adduct (**13**):* ^{1}H NMR (CD_3OD, 300 MHz): characteristic signals for **1**, δ_H 7.78, 6.75, 3.94, 3.89, and 1.91; characteristic signals for peptide, δ_H 7.18-7.35, 3.53-4.75, 2.15, 1.52-1.78, 1.10-1.50, and 0.90; ESITOF MS: *m/z* 1240.5500 $[M+H]^+$ (calcd for $C_{58}H_{82}N_9O_{19}S$, 1240.5448).

*1-Peptide Adduct (**14**):* ^{1}H NMR (CD_3OD, 300 MHz): characteristic signals for **1**, δ_H 7.79, 6.74, 3.95, 3.87, and 1.90; characteristic signals for peptide, δ_H 7.20-7.30, 3.52-4.65, 1.60, 1.30, 1.13, and 0.90; ESITOF MS: *m/z* 1256.5398 $[M+H]^+$ (calcd for $C_{58}H_{82}N_9O_{20}S$, 1256.5397).

Assay for Cytotoxic Activity

The isolated compounds **1**-**8** were evaluated for cytotoxic activity. The cytotoxicity against HuCCA-1, HepG2, A549, HeLa, T47D, MDA-MB231, and MRC-5 cell lines was assessed with MTT assay,[48] while the activity toward non-adhesive cells, HL-60 and MOLT-3 cell lines, was evaluated with XTT assay.[49] Purity of compounds **1**-**8** was >97% (by HPLC, as well as by ^{1}H and ^{13}C NMR spectra). The reference drugs were etoposide and doxorubicin, and the IC_{50} values of both drugs are provided in Table 2.

Conclusions

Eight fungal metabolites (**1**-**8**) were isolated from the mangrove endophytic fungus, *P. chermesinum*; among them, five compounds (**2**-**5** and **8**) were new natural products. Penicilliumolide A (**2**) was a novel tetracyclic polyketide, whose structure was uniquely spiro-attached with a γ-lactone ring. Compounds **1** and **6** exhibited potent cytotoxic activity, and they had selective cytotoxicity toward certain cancer cell lines. Compound **1** exhibited comparable cytotoxic activity toward T47D and MDA-MB231 cancer cell lines to that of doxorubicin, and its activity toward HepG2 cell line was more potent than etoposide. While TMC-264 (**1**) exhibited potent cytotoxic activity, its derivatives **2**–**5** did not possess the activity, therefore, the cytotoxicity of **1** was likely due to the β-chloro substituted α,β-unsaturated ketone functionality. It was found that **1** reacted with GSH, forming **1**-GSH adduct (**9**) in phosphate buffer, therefore, the β-chloro substituted α,β-unsaturated ketone of **1** is a thiol-reactive scaffold. TMC-264 (**1**) could also react with peptides containing cysteine, and it had different reactivity toward individual peptide. The thiol-reactive pharmacophore of **1** might be applicable to the drug design for glutathione modulation agents, fragment-based drug discovery for the design of irreversible enzyme inhibitors, bioconjugation, and click reaction. The facile C-S bond formation in water inspired by the natural product **1** could also be useful for green chemical synthesis.

Acknowledgements

This work is supported by the Center of Excellence on Environmental Health and Toxicology, Science & Technology Postgraduate Education and Research Development Office (PERDO), Ministry of Education. This research is also partially supported by Mahidol University. C. D. is grateful to the ASEAN Foundation and the Thailand International Development Cooperation Agency (TICA) for a student grant. We thank P. Intachote, S. Sengsai, and B. Saimanee for cytotoxicity testing.

Notes and references

1 M. Hagel, D. Niu, T. St Martin, M. P. Sheets, L. Qiao, H. Bernard, R. M. Karp, Z. Zhu, M. T. Labenski, P. Chaturvedi, M. Nacht, W. F. Westlin, R. C. Petter and J. Singh, *Nat. Chem. Biol.*, 2011, **7**, 22-24.

2 (a) M. H. Potashman and M. E. Duggan, *J. Med. Chem.*, 2009, **52**, 1231-1246; (b) R. Mah, J. R. Thomas and C. M. Shafer, *Bioorg. Med. Chem. Lett.*, 2014, **24**, 33-39; (c) N. R. Roqué Rosell, L. Mokhlesi, N. E. Milton, T. R. Sweeney, P. A. Zunszain, S. Curry and R. J. Leatherbarrow, *Bioorg. Med. Chem. Lett.*, 2014, **24**, 490-494.

3 L. V. Sequist, J. C. Yang, N. Yamamoto, K. O'Byrne, V. Hirsh, T. Mok, S. L. Geater, S. Orlov, C. M. Tsai, M. Boyer, W. C. Su, J. Bennouna, T. Kato, V. Gorbunova, K. H. Lee, R. Shah, D. Massey, V. Zazulina, M. Shahidi and M. Schuler, *J. Clin. Oncol.*, 2013, **31**, 3327-3334.

4 J. C. Byrd, R. R. Furman, S. E. Coutre, I. W. Flinn, J. A. Burger, K. A. Blum, B. Grant, J. P. Sharman, M. Coleman, W. G. Wierda, J. A. Jones, W. Zhao, N. A. Heerema, A. J. Johnson, J. Sukbuntherng, B. Y. Chang, F. Clow, E. Hedrick, J. J. Buggy, D. F. James and S. O'Brien, *N. Engl. J. Med.*, 2013, **369**, 32-42.

5 A. J. Smith, X. Zhang, A. G. Leach and K. N. Houk, *J. Med. Chem.*, 2009, **52**, 225-233.

6 (a) S. Krishnan, R. M. Miller, B. Tian, R. D. Mullins, M. P. Jacobson and J. Taunton, *J. Am. Chem. Soc.*, 2014, **136**, 12624-12630; (b) J. C. Collins, A. Armstrong, K. L. Chapman, H. C. Cordingley, A. A. Jaxa-Chamiec, K. E. Judd, D. J. Mann, K. A. Scott, C. J. Tralau-Stewart and C. M. R. Low, *Med. Chem. Commun.*, 2013, **4**, 1148-1155.

7 X. Tan, C. Bertonati, L. Qin, L. Furio, C. El Amri, A. Hovnanian, M. Reboud-Ravaux and B. O. Villoutreix, *Eur. J. Med. Chem.*, 2013, **70**, 661-668.

8 I. M. Serafimova, M. A. Pufall, S. Krishnan, K. Duda, M. S. Cohen, R. L. Maglathlin, J. M. McFarland, R. M. Miller, M. Frodin and J. Taunton, *Nat. Chem. Biol.*, 2012, **8**, 471-476.

9 C. Carmi, M. Mor, P. G. Petronini and R. R. Alfieri, *Biochem. Pharmacol.*, 2012, **84**, 1388-1399.

10 M. Yoshida, M. Kijima, M. Akita and T. Beppu, *J. Biol. Chem.*, 1990, **265**, 17174-17179.
11 L. M. Butler, D. B. Agus, H. I. Scher, B. Higgins, A. Rose, C. Cordon-Cardo, H. T. Thaler, R. A. Rifkind, P. A. Marks and V. M. Richon, *Cancer. Res.*, 2000, **60**, 5165-5170.
12 P. A. Marks and R. Breslow, *Nat. Biotechnol.*, 2007, **25**, 84-90.
13 R. Furumai, A. Matsuyama, N. Kobashi, K. H. Lee, M. Nishiyama, H. Nakajima, A. Tanaka, Y. Komatsu, N. Nishino, M. Yoshida and S. Horinouchi, *Cancer Res.*, 2002, **62**, 4916-4921.
14 J. Hong and H. Luesch, *Nat. Prod. Rep.*, 2012, **29**, 449-456.
15 D. L. Boger, C. W. Boyce, R. M. Garbaccio and J. A. Goldberg, *Chem. Rev.*, 1997, **97**, 787-828.
16 A. L. Wolfe, K. K. Duncan, N. K. Parelkar, D. Brown, G. A. Vielhauer and D. L. Boger, *J. Med. Chem.*, 2013, **56**, 4104-4115.
17 M. S. Tichenor, K. S. MacMillan, J. S. Stover, S. E. Wolkenberg, M. G. Pavani, L. Zanella, A. N. Zaid, G. Spalluto, T. J. Rayl, I. Hwang, P. G. Baraldi and D. L. Boger, *J. Am. Chem. Soc.*, 2007, **129**, 14092-14099.
18 S. Kusari, S. P. Pandey and M. Spiteller, *Phytochemistry*, 2013, **91**, 81-87.
19 R. X. Tan and W. X. Zou, *Nat. Prod. Rep.*, 2001, **18**, 448-459.
20 Y. Liu, S. Chen, Z. Liu, Y. Lu, G. Xia, H. Liu, L. He and Z. She, *Mar. Drugs*, 2015, **13**, 3091-3102.
21 C. M. Deng, S. X. Liu, C. H. Huang, J. Y. Pang and Y. C. Lin, *Mar. Drugs*, 2013, **11**, 2616-2624.
22 K. Tatsuta, A. Furuyama, T. Yano, Y. Suzuki, T. Ogura and S. Hosokawa, *Tetrahedron Lett.*, 2008, **49**, 4036-4039.
23 M. Sakurai, M. Nishio, K. Yamamoto, T. Okuda, K. Kawano and T. Ohnuki, *Org. Lett.*, 2003, **5**, 1083-1085.
24 R. D. Wei, H. K. Schnoes, P. A. Hart and F. M. Strong, *Tetrahedron*, 1975, **31**, 109-114.
25 A. Lin, G. Wu, Q. Gu, T. Zhu and D. Li, *Arch. Pharm. Res.*, 2014, **37**, 839-844.
26 Y. Moule, M. Jemmali and N. Rousseau, *Chem. Biol. Interact.*, 1976, **14**, 207-216.
27 S. Amslinger, *ChemMedChem*, 2010, **5**, 351-356.
28 (a) H. R. Kim, H. J. Lee, Y. J. Choi, Y. J. Park, Y. Woo, S. J. Kim, M. H. Park, H. W. Lee, P. Chun, H. Y. Chung and H. R. Moon, *Med. Chem. Commun.*, 2014, **5**, 1410-1417; (b) H. Y. Park Choo, K. H. Peak, J. Park, D. H. Kim and H. S. Chung, *Eur. J. Med. Chem.*, 2000, **35**, 643-648.
29 S. Gunnarsdottir and A. A. Elfarra, *J. Pharmacol. Exp. Ther.*, 1999, **290**, 950-957.
30 P. Ruzza, A. Rosato, A. Nassi, M. Rondina, M. Zorzin, C. R. Rossi, M. Floreani and L. Quintieri, *J. Med. Chem.*, 2009, **52**, 4973-4976.
31 G. K. Balendiran, R. Dabur and D. Fraser, *Cell Biochem. Funct.*, 2004, **22**, 343-352.
32 A. L. Ortega, S. Mena and J. M. Estrela, *Cancers*, 2011, **3**, 1285-1310.
33 J. Singh, R. C. Petter and A. F. Kluge, *Curr. Opin. Chem. Biol.*, 2010, **14**, 475-480.
34 D. E. Scott, A. G. Coyne, S. A. Hudson and C. Abell, *Biochemistry*, 2012, **51**, 4990-5003.
35 S. G. Kathman, Z. Xu and A. V. Statsyuk, *J. Med. Chem.*, 2014, **57**, 4969-4974.
36 A. C. Obermeyer, J. B. Jarman and M. B. Francis, *J. Am. Chem. Soc.*, 2014, **136**, 9572-9579.
37 S. L. Capehart, A. M. ElSohly, A. C. Obermeyer and M. B. Francis, *Bioconjug. Chem.*, 2014, **25**, 1888-1892.
38 (a) R. M. Stolz and B. H. Northrop, *J. Org. Chem.*, 2013, **78**, 8105-8116; (b) L. Markey, S. Giordani and E. M. Scanlan, *J. Org. Chem.*, 2013, **78**, 4270-4277; (c) A. Štorha, E. A. Mun and V. V. Khutoryanskiy, *RSC Adv.*, 2013, **3**, 12275-12279; (d) J. L. Huang, C. J. Li and D. G. Gray, *RSC Adv.*, 2014, **4**, 6965-6969.
39 (a) S. T. S. Chan, M. A. Pullar, I. M. Khalil, E. Allouche, D. Barker and B. R. Copp, *Tetrahedron Lett.*, 2015, **56**, 1486-1488; (b) A. Pansanit, N. Ingavat, T. Aree, C. Mahidol, S. Ruchirawat and P. Kittakoop, *Tetrahedron Lett.*, 2012, **53**, 2129-2131.
40 (a) C. Shen, P. Zhang, Q. Sun, S. Bai, T. S. Hor and X. Liu, *Chem. Soc. Rev.*, 2015, **44**, 291-314; (b) Y. Liu, B. Huang, X. Cao, D. Wu and J. P. Wan, *RSC Adv.*, 2014, **4**, 37733-37737; (c) W. Zhao, P. Xie, Z. Bian, A. Zhou, H. Ge, B. Niu and Y. Ding, *RSC Adv.*, 2015, **5**, 59861-59864.
41 M. Sakurai, M. Nishio, K. Yamamoto, T. Okuda, K. Kawano and T. Ohnuki, *J. Antibiot.*, 2003, **56**, 513-519.
42 C. M. Visagie, J. Houbraken, J. C. Frisvad, S. B. Hong, C. H. Klaassen, G. Perrone, K. A. Seifert, J. Varga, T. Yaguchi and R. A. Samson, *Stud. Mycol.*, 2014, **78**, 343-371.
43 T. J. White, T. Bruns, S. Lee and J. Taylor, in *PCR Protocols: A Guide to Methods and Applications*, eds. M. A. Innis, D. H. Gelfand, J. J. Sninsky and T. J. White, Academic Press, San Diego, 1990, pp. 315-322.
44 Z. Zhang, S. Schwartz, L. Wagner and W. Miller, *J. Comput. Biol.*, 2000, **7**, 203-214.
45 J. Houbraken, C. M. Visagie, M. Meijer, J. C. Frisvad, P. Busby, J. I. Pitt, K. A. Seifert, G. Louis-Seize, R. Demirel, N. Yilmaz, K. Jacobs, M. Christensen and R. A. Samson, *Stud. Mycol.*, 2014, **78**, 373-451.
46 H. Huang, X. Feng, Z. Xiao, L. Liu, H. Li, L. Ma, Y. Lu, J. Ju, Z. She and Y. Lin, *J. Nat. Prod.*, 2011, **74**, 997-1002.
47 S. W. Peterson, F. E. Vega, F. Posada and C. Nagai, *Mycologia*, 2005, **97**, 659-666.
48 J. Carmichael, W. G. DeGraff, A. F. Gazdar, J. D. Minna and J. B. Mitchell, *Cancer Res.*, 1987, **47**, 936-942.
49 A. Doyle and J. B. Griffiths, *Mammalian Cell Culture: Essential Techniques*, John Wiley & Sons, Chichester, UK, 1997.